Anal. Chem. **1999,** *71,* 3311−3317

Articles

Reactive Ion Scattering from Surfaces Bearing Isomeric Chlorinated Adsorbates

T. Pradeep,*,† Jianwei Shen, Chris Evans, and R. G. Cooks*

Department of Chemistry, Purdue University, West Lafayette, Indiana 47907

The value of low-energy ionic collisions for selective surface analysis is shown by the fact that reactive scattering allows differentiation of isomeric chemisorbates. Reactions of $Cr^{\bullet+}$ and Cr-containing cations at chlorobenzyl mercaptan (CBM) monolayers on Au surfaces show different reaction products, depending on the position of chlorine substitution in the phenyl ring. The chlorine atom abstraction product, $CrCl^+$, is observed at 45-eV collision in 4-CBM and is completely absent in 2-CBM at the same energy. The sensitivity of reactive ion scattering to the isomeric adsorbate is further demonstrated by the fact that the peak corresponding to $Cr^{\bullet+}$ addition and Cl loss via Cl−C bond cleavage, $C_7H_6SCr^+$, is large in the monolayer formed from 4-CBM, but weak in the 2-CBM monolayer, suggesting that the chlorine is below the first layer of atoms in the latter case. The inverse intensity relationship applies for the dehydrohalogenation product $C_7H_5Cr^+$ where the Cl atom at the ortho position in 2-CBM facilitates the intramolecular elimination of HCl. The 85-eV $Xe^{\bullet+}$ chemical sputtering mass spectra are the same for both surfaces, indicating similarities in the electron-transfer and momentum-transfer processes. A related set of isomers, 2-, 3- and 4-chlorothiophenol, chemisorbed on gold, shows no differences in ion/surface reactions or chemical sputtering.

Ionic reactions at molecular surfaces represent an emerging area of chemistry with implications for materials science, mass spectrometry, and surface science including selective surface transformations. Apart from its potential applications, fundamental aspects of this chemistry are also beginning to attract attention due to the variety and diversity of the processes involved.[1,2] These experiments parallel reactive scattering of molecular beams.[3−5] Ion/surface reactions can be carried out with a wide range of (ionic) chemical reagents and over a wide range of impact energies. Key issues, such as the degree of thermochemical control of the observed processes,[6−9] the interfacial reaction dynamics and mechanism,[10−15] and the role of electron transfer in reactive scattering,[7,16−18] are being pursued actively. Efforts have been made to acquire insights into the reaction dynamics, including the time scale of the ion/surface interaction, the energy partitioning upon collision, angular effects,[11,19−22] and excited-state effects.[23−26] The discovery of new reactions and understanding of the molecular details of the processes by performing analogous

† Fulbright Fellow, on leave from the Department of Chemistry and Regional Sophisticated Instrumentation Center, Indian Institute of Technology, Madras 600 036, India.

(1) Cooks, R. G.; Ast, T.; Pradeep, T.; Wysocki, V. *Acc. Chem. Res.* **1994**, *27*, 316−323.
(2) Kasi, S. R.; Kang, H.; Sass, C. S.; Rabalais, J. W. *Surf. Sci. Rep.* **1989**, *10*, 1.
(3) Ferkel, H.; Singleton, J. T.; Reisler, H.; Wittig, C. *Chem. Phys. Lett.* **1994**, *221*, 447.
(4) Arnold, D. W.; Korolik, M.; Wittig, C.; Reisler, H. *Chem. Phys. Lett.* **1998**, *282*, 313.
(5) Arumainayagam, C. R.; Madix, R. J. *Prog. Surf. Sci.* **1991**, *38*, 1.
(6) Morris, M. R.; Riederer, D. E., Jr.; Winger, B. E.; Cooks, R. G.; Ast, T.; Chidsey, C. E. D. *Int. J. Mass Spectrom. Ion Processes* **1992**, *122*, 181.
(7) Hayward, M. J.; Park, F. D. S.; Phelan, L. M.; Bernasek, S. L.; Somogyi, A.; Wysocki, V. H. *J. Am. Chem. Soc.* **1996**, *118*, 8375.
(8) Shen, J.; Grill, V.; Cooks, R. G. *J. Am. Chem. Soc.* **1998**, *120*, 4254−4255.
(9) de Maaijer-Gielbert, J.; Somogyi, A.; Wysocki, V. H.; Kistemaker, P. G.; Weeding, T. L. *Int. J. Mass Spectrom.* **1998**, *174*, 81−94.
(10) Pradeep, T.; Ast, T.; Cooks, R. G.; Feng, B. *J. Phys. Chem.* **1994**, *98*, 9301.
(11) Pradeep, T.; Riederer, D. E., Jr.; Hoke, II. S. H.; Ast, T.; Cooks, R. G.; Linford, M. R. *J. Am. Chem. Soc.* **1994**, *116*, 8658.
(12) Williams, E. R.; Jones, G. C., Jr.; Fang, L.; Zare, R. N.; Garrison, B. J.; Brenner, D. W. *J. Am. Chem. Soc.* **1992**, *114*, 3207−3210.
(13) Cooks, R. G.; Ast, T.; Mabud, Md. A. *Int. J. Mass Spectrom. Ion Processes* **1990**, *100*, 209−265.
(14) Dongre, A. R.; Somogyi, A.; Wysocki, V. H. *J. Mass Spectrom.* **1996**, *31*, 339.
(15) Burroughs, J. A.; Wainhaus, S. B.; Hanley, L. *J. Chem. Phys.* **1995**, *103*, 6706.
(16) Ast, T.; Pradeep, T.; Feng, B.; Cooks, R. G. *J. Mass Spectrom.* **1996**, *31*, 791−801.
(17) Hayward, M. J.; Park, F. D. S.; Phelan, L. M.; Bernasek, S. L.; Somogyi, A.; Wysocki, V. H. *J. Am. Chem. Soc.* **1996**, *118*, 8375.
(18) Kang, H.; Kim, K. D.; Kim, K. Y. *J. Am. Chem. Soc.* **1997**, *119*, 12002−12003.
(19) Koppers, W. R.; Tsumori, K.; Beijersbergen, J. H. M.; Weeding, T. L.; Kistemaker, P. G.; Kleyn, A. W. *Int. J. Mass Spectrom.* **1998**, *174*, 11−34.
(20) Koppers, W. R.; Beijersbergen, J. H. M.; Weeding, T. L.; Kistemaker, P. G.; Kleyn, A. W. *J. Chem. Phys.* **1997**, *107*, 10736−10750.
(21) Morris, J. R.; Martin, J. S.; Greeley, J. N.; Jacobs, D. C. *Surf. Sci.* **1995**, *330*, 323−336.
(22) Mair, C.; Fiegele, T.; Wörgötter, R.; Futrell, J. H.; Märk, T. D. *Int. J. Mass Spectrom.* **1998**, *177*, 105.
(23) Worgotter, R.; Grill, V.; Herman, Z.; Schwarz, H.; Märk, T. D. *Chem. Phys. Lett.* **1997**, *270*, 333−338.
(24) Schultz, D. G.; Wainhaus, S. B.; Hanley, L.; deSainteClaire, P.; Hase, W. L. *J. Chem. Phys.* **1997**, *106*, 10337−10348.
(25) Shen, J.; Grill, V.; Evans, C.; Cooks, R. G. *J. Mass Spectrom.*, in press.
(26) Miller, S. A.; Riederer, D. E.; Cooks, R. G.; Cho, W. R.; Lee, H. W.; Kang, H. *J. Phys. Chem. US* 1994, *98*, 245−251.

10.1021/ac990402t CCC: $18.00 © 1999 American Chemical Society
Published on Web 06/30/1999

ion/molecule reactions[27,28] have widened the scope of this area.

The interaction region for low collision energies (<100-eV laboratory system) is limited to the topmost surface atoms, and the ion/surface reactions are localized to the vicinity of the collision site.[11,23,29,30] Furthermore, it is known that chemical effects control the ionization and ejection of organic groups through the process of low-energy chemical sputtering.[31] We suggest that changes in adsorbate structure should be recognizable in the products of ion/surface chemistry using appropriate reagent ions. In particular, it should be possible to detect differences in isomeric structures of the adsorbate by reactive collisions. This study is an attempt to investigate this possibility using well-organized surfaces, the self-assembled monolayers.[32] We show that ion/surface processes—including reactions and chemical sputtering—in certain cases do reflect differences in the adsorbate chemical structure even when the changes are as subtle as those investigated here, viz. positional isomerization on an aromatic ring. It has been demonstrated by Gu and Wysocki[29] that in the case of 30-eV collisions of benzene molecular ions upon an isotopically labeled Langmuir−Blodgett (LB) film of $^{13}CH_3(CH_2)_{16}COOH$ or $CD_3(CH_2)_{16}COOH$, it is predominantly the terminal CH_3 group that is abstracted. Their study elegantly demonstrates the extreme surface sensitivity of ion/surface reactions but does not explore the isomeric distinction, which we tackle in this paper. Note too, that the related issue of adsorbate geometry is encountered in this study—there is little direct evidence of the geometry as opposed to the connectivity of the adsorbate but the results obtained are intepreted as revealing features of these three-dimensional structures.

The binding sites of alkanethiols on gold surfaces are well understood from a number of studies. On a (111) gold surface, sulfur binds in a $(\sqrt{3} \times \sqrt{3})R30°$ overlayer.[33] A c (4×2) superlattice of the $(\sqrt{3} \times \sqrt{3})R30°$ hexagonal lattice has also been seen in scanning tunneling microscopy (STM) and grazing incidence X-ray diffraction studies.[34−36] In this geometry, the sulfur atoms have nearest-neighbor distances of 5.2 Å and next-nearest-neighbor distances of ∼9 Å. The adsorbate geometry has been elucidated for a number of aromatic thiol systems[37] and for alkanethiols with aromatic groups.[38,39] Most of these studies have been performed with Raman spectroscopy, especially surface-enhanced Raman scattering (SERS), but grazing incidence infrared spectroscopy and scanning tunneling and atomic force microscopies have also been used. A large number of Raman studies has been performed on Ag surfaces and Ag colloidal particles due to their high SERS activity,[40,41] and there have been investigations on Au surfaces as well.[42−44] Oligo(phenylethynyl)-benzenethiols on gold surfaces have been shown to give a $(\sqrt{3} \times \sqrt{3})R30°$ overlayer[45] as well as a $(2\sqrt{3} \times \sqrt{3})R30°$ overlayer.[37] Structural studies have also been extended to understand molecular orientation at surfaces,[46] including adsorption of diphenyl sulfide, diphenyl disulfide, and dibenzyl disulfide on Ag and Au surfaces.[47,48] SERS studies suggest that, on a silver surface, phenyl species "lie flat", whereas the benzyl species is "sticking up" from the surface. The strong phenyl ring−surface π interaction is probably responsible for the flat absorption geometry.[47]

Five commercially available chloro-substituted aromatic thiols were used in this study, including 4-chlorobenzyl mercaptan (4-CBM), 2-chlorobenzyl mercaptan (2-CBM), 4-chlorothiophenol (4-CTP), 3-chlorothiophenol (3-CTP), and 2-chlorothiophenol (2-CTP). Although their geometries (as opposed to their connectivities) are not known independently, the above arguments are expected to apply to the self-assembled monolayers (SAMs) of 4-CBM and 2-CBM on gold. The van der Waals cross section of the molecules is small so that they can be accommodated in a $(\sqrt{3} \times \sqrt{3})R30°$ structure.[49] This was demonstrated earlier with monolayers of $C_6H_5-C\equiv C-C_6H_4-C\equiv C-C_6H_4-SH$ on Au where diphenylacetylene units replace the normal hydrocarbon chain.[50] Thus, adsorbed 4-CBM is expected to be orientated with the chlorine atom exposed to the vacuum interface while in 2-CBM the chlorine atom is below the first atoms of adsorbate (Figure 1). In contrast to the benzyl mercaptan system, 2-, 3-, and 4-CTP are expected to form poor monolayers on gold with rather disordered structures and low packing density.[51] STM images showed that thiophenols form a $(\sqrt{3} \times \sqrt{3})R30°$ overlayer in only a few occasions. The domain size is as small as ∼4 nm.[51] The insertion of the CH_2 unit between the aromatic ring and the sulfur atom is important to relax the rigidity of the thiol headgroup and it also facilitates intermolecular interactions.[51] A further objective of the experiments outlined below was therefore directed toward seeing whether the effects of this structural difference can be observed in ion/surface reactive collisions. Although ion/surface inelastic collisions have been used to distinguish isomeric ions[52,53] by analysis of their dissociation patterns, the differentiation of

(27) Lim, H.; Schultz, D. G.; Gislason, E. A.; Hanley, L. *J. Phys. Chem. B* **1998**, *102*, 4573.
(28) Chen, G.; Hoke, S. H.; II, Cooks, R. G. *Int. J. Mass Spectrom. Ion Processes* **1994**, *139*, 87−93.
(29) Patrick, J.; Pradeep, T.; Luo, H.; Ma, S.; Cooks, R. G. *J. Am. Soc. Mass Spectrom.* **1998**, *9*, 1158−1167.
(30) Gu, C.; Wysocki, V. H. *J. Am. Chem. Soc.* **1997,** *119*, 12010−12011.
(31) Schultz, D. G.; Wainhaus, S. B.; Hanley, L.; de Sainte Claire, P.; Hase, W. L. *J. Chem. Phys.* **1997**, *106*, 10337−10348.
(32) Pradeep, T.; Evans, C.; Shen, J.; Cooks, R. G. *J. Phys. Chem. A*, in press.
(33) Vincenti, M.; Cooks, R. G. *Org. Mass Spectrom.* **1988**, *23*, 317.
(34) Ulman, A. *An Introduction to Ultrathin Organic Films*; Academic Press: Boston, 1991.
(35) Gu, C.; Wysocki, V. H. *J. Am. Chem. Soc.* **1997**, *119*, 12010−12011.
(36) Ulman, A. *Chem. Rev.* **1996**, *96*, 1533.
(37) Delamarche, E.; Michel, B.; Gerber, C.; Anselmetti, D.; Guntherodt, H.-J.; Ringsdorf, H. *Langmiur* **1995**, *10*, 2869.
(38) Kim, Y.-T.; McCarley, R. L.; Bard, A. J. *J. Phys. Chem.* **1992**, *96*, 7416.
(39) Schreiber, F.; Eberhardt, A.; Leung, T. Y. B.; Schwartz, P.; Wetterer, S. M.; Lavrich, D. J.; Berman, L.; Fenter, P.; Eisenberger, P.; Scoles, G. *Phys. Rev. B* **1998**, *57*, 12476−12481.
(40) Dhirani, A.-A.; Zehner, R. W.; Hsung, R. P.; Guyot-Sionnest, P.; Sita, L. R. *J. Am. Chem. Soc.* **1996**, *118*, 3319.
(41) Gui, J. Y.; Stern, D. A.; Frank, D. G.; Liu, F.; Zapien, D. C.; Hubbard, A. T. *Langmiur* **1991,** *7*, 955.
(42) Gui, J. Y.; Stern, D. A.; Hubbard, A. T. *J. Electroanal. Chem.* **1990**, *292*, 245.
(43) (a) Chang, R. K., Furtak, T. E., Eds. *Surface Enhanced Raman Scattering*; Plenum Press: New York, 1982. (b) Suetaka, W. *Surface Infrared and Raman Spectroscopy*; Plenum Press: New York, 1995.
(44) (a) Gao, X.; Davies, J. P.; Weaver, M. J. *J. Phys. Chem.* **1990**, *94*, 6858. (b) Gao, P.; Weaver, M. J. *J. Phys. Chem.* **1985**, *89*, 5040.
(45) Bryant, M. A.; Pemberton, J. E. *J. Am. Chem. Soc.* **1991**, *113*, 8284.
(46) Sabatani, E.; Cohen-Boulakia, J.; Bruening, M.; Rubinstein, I. *Langmuir* **1993**, *9*, 2974−2981.
(47) Murty, K. V. G. K.; Venkataramanan, M.; Pradeep, T. *Langmiur* **1998**, *14*, 5446.
(48) Sandroff, C. J.; Herschbach, D. R. *J. Phys. Chem.* **1982**, *86*, 3277−3279.
(49) Abduaini, A.; Kera, S.; Aoki, M.; Okudaira, K. K.; Ueno, N.; Harada, Y. *J. Electron Spectrosc. Relat. Phenom.* **1998**, *88*, 849−854.
(50) Poirier, G. E. *Chem. Rev.* **1997**, *97*, 1117.
(51) Dhirani, A.-A.; Zehner, R. W.; Hsung, R. P.; Guyot-Sionnest, P.; Sita, L. R. *J. Chem. Phys.* **1997**, *106*, 5249-.
(52) Tao, Y.-T.; Wu, C.-C.; Eu, J.-Y.; Lin, W.-L. *Langmuir* **1997**, *13*, 4018−4023.

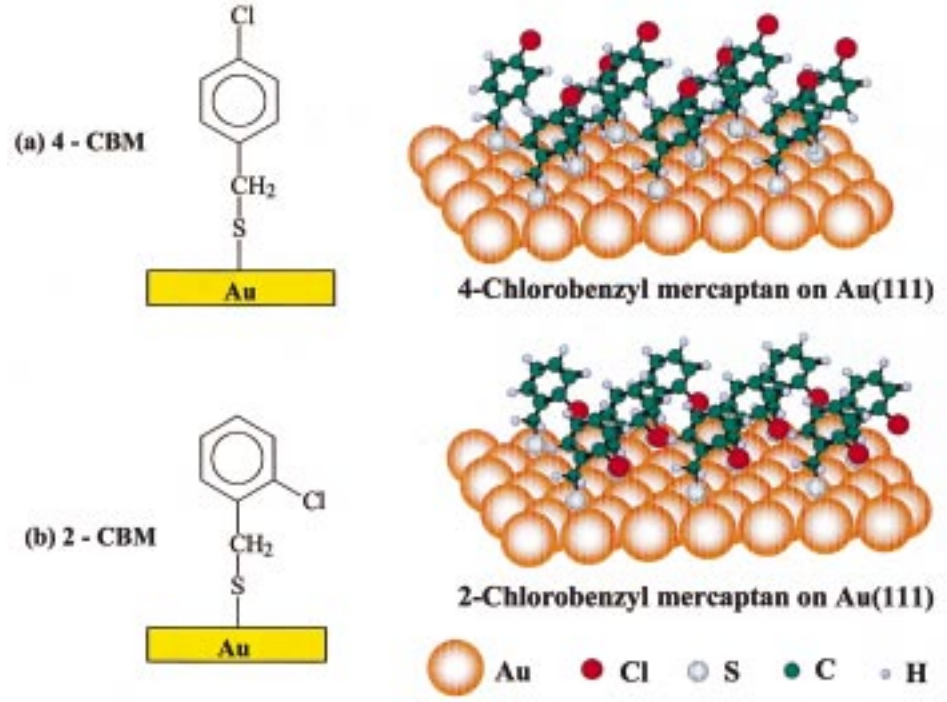

Figure 1. Schematic of the assumed adsorption geometries and known connectivities of (a) 4-CBM and (b) 2-CBM on an Au (111) surface. Sulfur is anchored on the 3-fold hollow sites giving a $(\sqrt{3} \times \sqrt{3})R30°$ lattice.

isomeric chemisorbates by reactive scattering is reported here for the first time.

EXPERIMENTAL SECTION

The monolayer samples were prepared by chemisorption from solution on a gold film vapor deposited (2000 Å) on optically polished glass plates with an adhesive 50-Å Cr buffer layer. The X-ray diffraction patterns (Seimens powder diffractometer with Cu Kα radiation) of these surfaces showed only gold (111) reflections as expected in view of the fact that this is the lowest energy surface of gold and thin film growth preferentially propagates in this direction. The surfaces were cleaned with piranha solution (H_2SO_4/H_2O_2, in 1:3 volume ratio) (caution: piranha solution is highly oxidizing and care should be taken in handling it). After exposure to the thiol solution, the surfaces were washed with ethanol repeatedly and dried in a stream of nitrogen and introduced into the spectrometer. Five thiols, 4-CBM, 2-CBM, 4-CTP, 3-CTP, and 2-CTP, were used to make the monolayer surfaces examined in this study. The surfaces were prepared by exposing a 1 mM solution of the corresponding thiol solution in ethyl alcohol to previously cleaned gold surfaces for 24 h. Preparation of SAMs is well documented in the literature.[32]

Typical measurement periods for the ion scattering experiments were on the order of several hours, and the ion doses involved were on the order of 10^{10} ions/cm^2. One does not expect significant surface damage from these fluences; i.e., the experiments are done under static conditions. A much longer ion beam exposure time is needed to effect significant modification to the monolayer.[54,55] Nevertheless, to minimize surface damage, different monolayers were used for each series of experiments. Also the sample position was varied periodically so that fresh surface was exposed to the ion beam.

Experiments were conducted using a four-analyzer BEEQ mass spectrometer described previously.[56] A mass- and energy-selected ion beam is directed from the BE analyzers to the surface held in an ultrahigh vacuum scattering chamber. The beam is decelerated to the chosen collision energy. The energy and mass distributions of the product ions are analyzed using the remaining EQ analyzers. In the experiments described, the scattering angle was set at 90°, the base pressure was 5×10^{-9} Torr, and the collision energy range investigated was 10−90 eV. Primary ions were generated by 70-eV electron impact on $Cr(CO)_6$ and Xe. All compounds were purchased from Aldrich and were used as received.

RESULTS AND DISCUSSION

The scattered ion mass spectra recorded upon collision of $Cr(CO)_6^{\bullet+}$ projectile ions on the isomeric adsorbates 4- and 2-CBM at 85-eV collision energy are compared in Figure 2. The most prominent features in the mass spectra appear at m/z 52 and 80 and are due to $Cr^{\bullet+}$ and $Cr(CO)^{\bullet+}$. Both are products of surface-induced dissociation (SID) of the projectile, that is, of inelastic scattering. It is seen that, at this collision energy, the higher metal carbonyl ions are completely absent, consistent with the large inelastic energy transfer expected.[6] It is known that ∼16% of the

(53) (a) Hayakawa, S.; Feng, B.; Cooks, R. G. *Int. J. Mass Spectrom.* **1997**, *167*, 525−539. (b) Schaaff, T. G.; Qu, Y.; Farrell, N.; Wysocki, V. H. *J. Mass Spectrom.* **1998**, *33*, 436−443.

(54) Kane, T. E.; Angelico, V. J.; Wysocki, V. H. *Anal. Chem.* **1995**, *67*, 1019−1019.

(55) Pradeep, T.; Feng, B.; Ast, T.; Patrick, J. S.; Cooks, R. G.; Pachuta, S. J. *J. Am. Soc. Mass Spectrom.* **1995**, *6*, 187−194.

(56) Winger, B. E.; Laue, H. J.; Horning, S. R.; Julian, R. K., Jr.; Lammert, S. A.; Riederer, D. E., Jr.; Cooks, R. G. *Rev. Sci. Instrum.* **1992**, *63*, 5613.

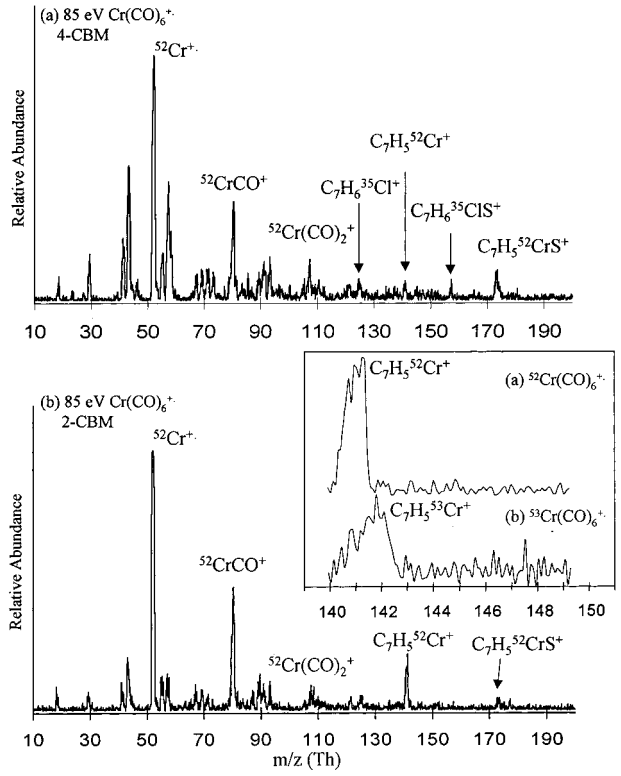

Figure 2. Scattered ion mass spectrum for collision of $Cr(CO)_6^{\bullet+}$ on chemisorbed (a) 4-CBM and (b) 2-CBM monolayers on Au at 85-eV collision energy. The peaks are assigned as labeled. Inset shows the scattered ion mass spectrum from 2-CBM in the *m*/*z* 141 region for (a) $^{52}Cr(CO)_6^{\bullet+}$ and (b) $^{53}Cr(CO)_6^{\bullet+}$.

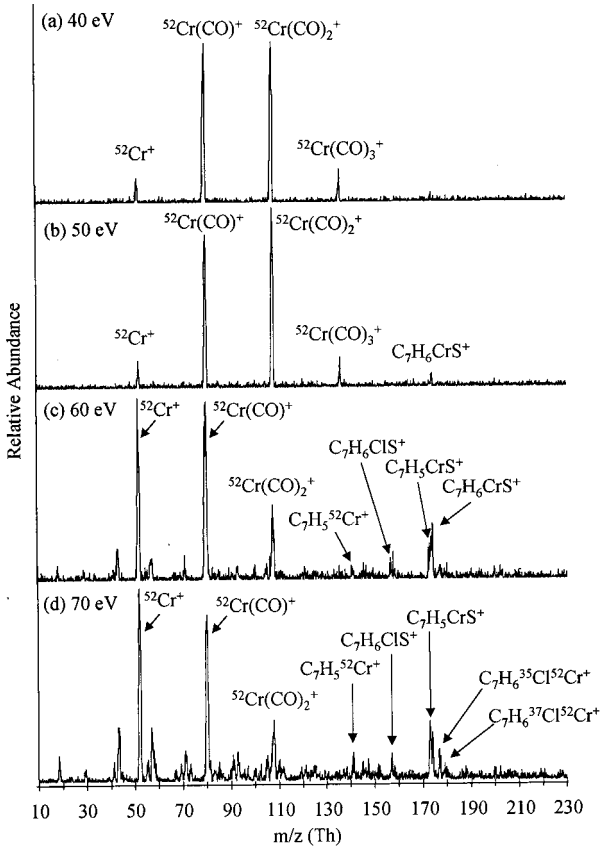

Figure 3. Scattered ion mass spectrum for collision of $Cr(CO)_6^{\bullet+}$ on chemisorbed 4-CBM monolayer surface on Au over a range of collision energies: (a) 40, (b) 50, (c) 60, and (d) 70 eV. Note the appearance of the peaks at *m*/*z* 173 and 141 assigned as $C_7H_5CrS^+$ and $C_7H_5Cr^+$, respectively.

translational energy of the projectile can be converted to the internal energy in the collisions with a hydrocarbon SAM surface.[6] Features are observed due to chemical sputtering of the surface species, i.e., due to electron transfer to the surface and release of ionized fragments of the adsorbate. Hydrocarbon ions ($C_xH_y^+$) with one to seven carbon atoms and varying numbers of hydrogens are represented. The overall pattern is noticeably different from the typical chemical sputtering pattern observed with hydrocarbon monolayers. One difference is the presence of the peaks at *m*/*z* 89 and 91. Another is that the maximum of the $C_xH_y^+$ abundance distribution is shifted to C_3-C_4 ions from C_2 ions, which is typical of a long-chain alkane SAM. The low abundance of C_2 hydrocarbon ions suggests that the surface is relatively free of hydrocarbon contaminants.

The higher mass region of the scattered ion spectrum contains ion/surface reaction products that are diagnostic of the adsorbate structure. Peaks of particular interest appear at *m*/*z* 141 and 173 and both these ions contain $Cr^{\bullet+}$ as revealed by isotopic labeling (see the inset of Figure 2). They are assigned as $C_7H_5Cr^+$ and $C_7H_5CrS^+$, respectively. Note that the peak *m*/*z* 173 is intense in 4-CBM whereas it is weak in 2-CBM. By contrast, the peak at *m*/*z* 141 is intense in 2-CBM but not in 4-CBM. In zoom scans not shown, both surfaces also display a feature at *m*/*z* 177/179, with the characteristic chlorine isotopic pattern, assigned as $C_7H_6ClCr^+$. Another important feature of the spectrum of the para absorbate is the peak at *m*/*z* 157, assigned as $C_7H_6ClS^+$ and virtually absent in the spectrum of the ortho isomer.

To confirm the assigned molecular formulas, experiments were performed over a range of collision energies. The scattered ion mass spectrum of $Cr(CO)_6^{\bullet+}$ recorded for the 4-CBM surface over a range of collision energies is shown in Figure 3. At 40-eV collision energy, the projectile ion undergoes inelastic collision leading to simple fragmentation; no reaction products are observed. As the collision energy is increased to 50 eV, the peak at *m*/*z* 173 is observed but *m*/*z* 174 is more intense while no signal is seen at *m*/*z* 141 or at *m*/*z* 177. As the collision energy is increased further, *m*/*z* 173 is favored relative to *m*/*z* 174, while at 60-eV collision energy, ions at *m*/*z* 141 and 177 appear. The peak at *m*/*z* 157 also appears in the spectrum at about this collision energy.

These experimental observations are consistent with the other data to be discussed later, if the ions of *m*/*z* 141, 173, 174, and 177 are assigned to $C_7H_5-Cr^+$, $C_7H_5S-Cr^+$, $C_7H_6S-Cr^+$, and $ClC_7H_6-Cr^+$, and the peak at *m*/*z* 157 is attributed to the intact ionized adsorbate, $ClC_6H_4CH_2S^+$. The origin of each of these peaks can be explained as a result of simple bond cleavages and elimination reactions illustrated in Scheme 1. The structures of the ions indicated there are only tentative, given the possibility of ring expansion and other isomeric forms of the gas-phase ions. Upon collision of $Cr(CO)_6^{\bullet+}$ with the surface, chemical sputtering of the surface species can occur and this explains the ionized benzyl sulfide peak at *m*/*z* 157. It is likely that this desorbed species dissociates further, explaining some of the lower mass ions (compare Figure 2a). Ion/surface reactions appear to give rise to many of the other products. The formation of the *m*/*z* 177

Scheme 1

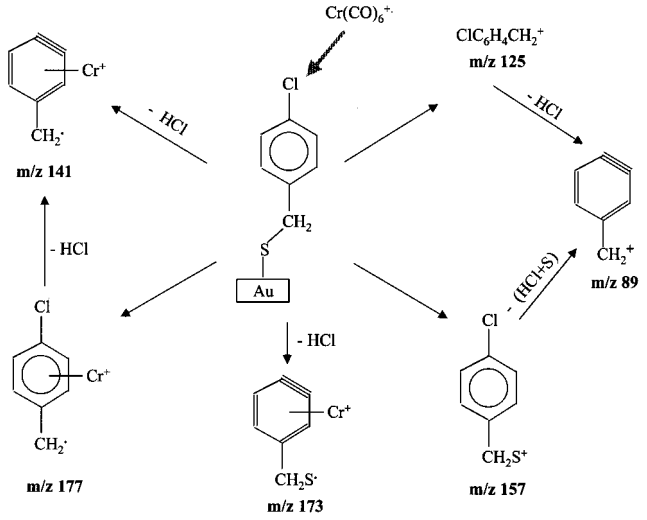

Scheme 2

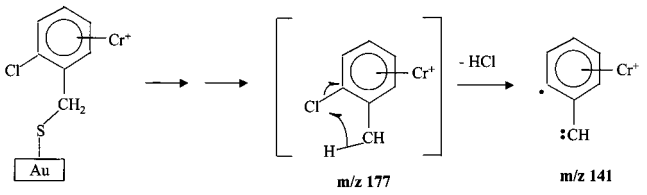

ion results from the simple process of benzyl−sulfur cleavage and attachment of $Cr^{\bullet+}$ to the aromatic fragment. Reaction of Cr^+ with the intact adsorbate followed by the loss of Cl explains the peak at m/z 174. The fact that the peak at m/z 173 is favored at higher collision energies suggests that this loss of hydrogen and chlorine atoms can occur independently. The ion at m/z 141 is explained as a result of fragmentation by loss of HCl from m/z 177.

The intensity variation among this set of ions changes with the isomeric form of the adsorbate, and this surface adsorbate isomer specificity is the principal finding of this study. It is interesting to note that even though the formation of these scattered product ions from both the 4- and 2-CBM surfaces involves the loss of chlorine atoms, they appear to occur by two completely different mechanisms, which are reflected in the relative abundance of the product ions. In the case of 2-CBM, the peak at m/z 141 ($C_7H_5-Cr^+$) is considerably more abundant than it is in 4-CBM. The formation of $C_7H_5-Cr^+$ involves an HCl loss through rearrangement, and this process is expected to be facilitated if the substituents are in the ortho position, as illustrated in Scheme 2. Note that this elimination process probably occurs during desorption. If the chlorine atoms are exposed to the surface and so directly interact with the incoming projectile ions, as in the case of para isomer, simple cleavage of the Cl−C bond occurs and results in the formation of $C_7H_6S-Cr^+$, as observed in the increased intensity of the peak at m/z 174. This again suggests that the low-energy ions interact primarily with the topmost atomic layers and these interactions appear to display remarkable stereochemical control. The difference in adsorbate structures shows up in those scattered ions that are associated with chemical sputtering also. This is seen in the fact that the intact ionized absorbate, m/z 157, is intense in 4-CBM but weak in 2-CBM. There is no reason to believe that 2-CBM would be bound to the

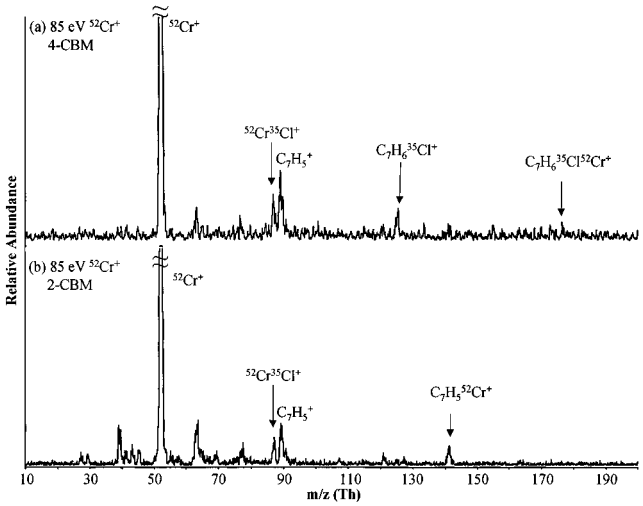

Figure 4. Scattered ion mass spectrum for collision of $Cr^{\bullet+}$ on chemisorbed (a) 4-CBM and (b) 2-CBM monolayers on Au at 85-eV collision energy.

surface more strongly than 4-CBM but the result is accommodated by the suggested facile HCl loss involving the benzylic hydrogen and an ortho chlorine atom.

After self-assembly, monolayers of 4-CBM and 2-CBM were examined using angle-resolved X-ray photelectron spectroscopy (XPS). The results of this analysis showed a systematic decrease of chlorine as the electron beam angle was increased on the 4-CBM monolayer. This is consistent with the chlorine atom projecting upward at the monolayer vacuum interface, as a shallower beam angle in analysis defines a shallower penetration of the electron beam into the monolayer. Conversely, the 2-CBM monolayer contained a smaller amount of accessible chlorine to the electron beam, with little variation as the beam angle was increased. Although these results may not be well defined, they support the assumptions made on the orientation of each monolayer.

Figure 4 shows the scattered ion mass spectra recorded upon collision of $^{52}Cr^{\bullet+}$ at 4-CBM and 2-CBM monolayers at 85-eV collision energy. The most important aspect of these spectra is the observation of a chlorine abstraction product ($CrCl^+$, m/z 87) from the 4-isomer where it is expected to be much more accessible to the reagent ion than in the 2-isomer (compare Figure 1). In addition to these peaks, ion/surface reaction products at m/z 141 ($C_7H_5Cr^+$) and 173 ($C_7H_5CrS^+$) are seen in the spectra. Confirming the observations made using $Cr(CO)_6^{\bullet+}$, the peak at m/z 141 is more intense in 2-CBM than in 4-CBM.

The collision energy dependence of chlorine abstraction by Cr^+ is substantially different for the isomeric CBM monolayers. In the case of 4-CBM, the peak at m/z 87 is still observable at 45-eV collision energy whereas the peak is absent in the spectrum of 2-CBM. This minor spectral feature is consistent with a proposed adsorbate geometry in which chlorine is present at the surface of 4-CBM whereas it is beneath the phenyl ring in the case of 2-CBM.

Figure 5 presents the chemical sputtering mass spectra recorded upon the collision of $Xe^{\bullet+}$ at the two isomeric surfaces. Both spectra are similar and show the same set of ions, including the structurally diagnostic doublet at m/z 125/127, attributed to $Cl-C_6H_4CH_2^+$. Note that this peak was also observed with both

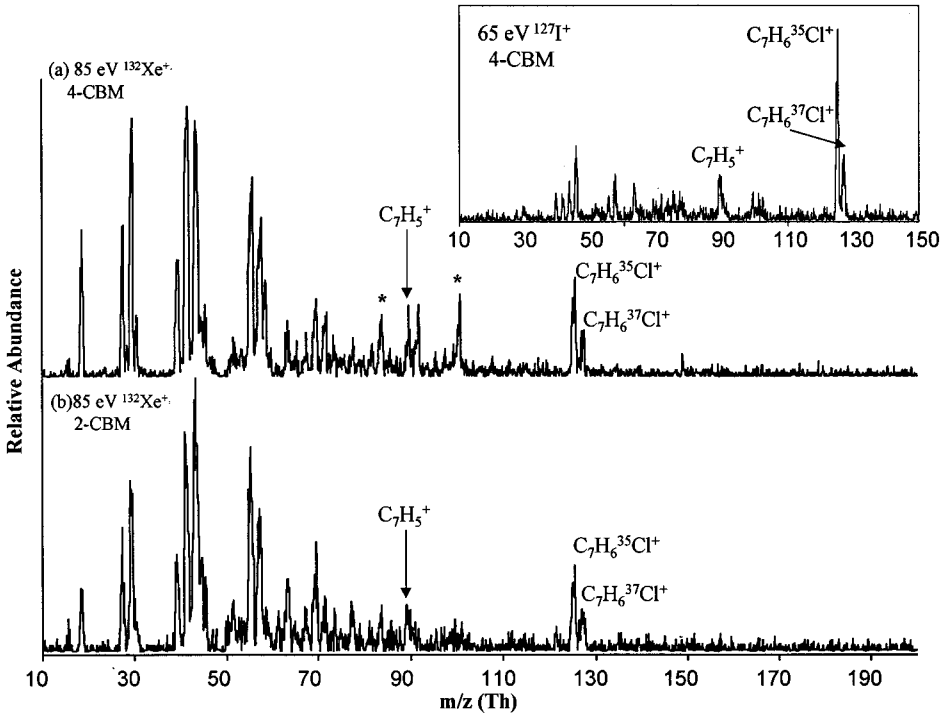

Figure 5. Scattered ion mass spectrum upon the collision of $Xe^{\bullet+}$ on chemisorbed (a) 4-CBM and (2) 2-CBM monolayers on Au at 85-eV collision energy. Inset shows the spectrum with I^+ projectile at 65-eV collision energy from a 4-CBM monolayer.

$Cr(CO)_6^+$ and $Cr^{\bullet+}$ projectiles, although in low abundance; $C_7H_5^+$ (m/z 89), a dissociation product by loss of HCl, is also observed. It is possible to increase the abundance of this ion by varying the nature of the projectile. For example, in a chemical sputtering mass spectrum recorded with $^{127}I^+$, it is the base peak (see the inset of Figure 5). This is also the case with projectiles such as CCl_3^+, $PCl_3^{\bullet+}$, and $I_2^{\bullet+}$, which do not exhibit reactive scattering as a competitive channel. One important difference between the $Xe^{\bullet+}$ chemical sputtering and the reactive scattering data is that while the $Cr^{\bullet+}$ reaction product shows an important ortho effect leading to the loss of HCl, the surface fragment, $Cl-C_6H_4-CH_2^+$ itself shows no such effect. The result is that simple chemical sputtering does not allow isomeric adsorbate differentiation in this case.

To compare the results with those of a similar system, we performed experiments with the same projectile ions on the monolayers of 2-, 3-, and 4-CTP on Au. In Figure 6, the scattered ion mass spectrum recorded for collision of $Cr^{\bullet+}$ at 85 eV on 4-CTP is shown. The characteristic features of the spectrum are the chlorine abstraction product $CrCl^+$ at m/z 87/89 and the ring abstraction product $Cr-C_6H_3^+$ at m/z 127, corresponding to the loss of HCl from $Cr-C_6H_4Cl^+$. Since the spectra from the isomeric adsorbates are identical, they are not presented. As mentioned in the introduction, thiophenols form much poorer monolayer structures on gold than do benzyl mercaptans. The lack of observable differences in reactive scattering between the isomeric CTP surfaces might be attributable simply to the fact that these surfaces possess poorly packed molecular structures.[51]

The scattered ion mass spectrum recorded upon collision of $Xe^{\bullet+}$ at the 4-CTP monolayer shows $C_2H_3^+$ (55%, relative abundance), $C_2H_5^+$(90), $C_3H_3^+$(25), $C_3H_5^+$(90), $C_3H_5^+$(100), $C_3H_7^+$(70), $C_4H_7^+$(40), $C_4H_9^+$(40), $C_5H_9^+$(27), and $C_5H_{11}^+$(23). Since the corresponding chemical sputtering spectra for the surfaces with

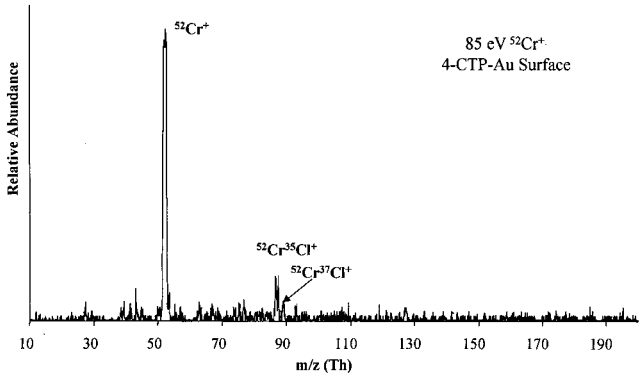

Figure 6. Scattered ion mass spectrum recorded upon the collision of $Cr^{\bullet+}$ on a 4-CTP monolayer surface at 85-eV collision energy.

the isomeric adsorbates are identical, they are not presented. The spectrum shows all the hydrocarbon fragments possible from such a surface, from C_1 to C_6. Neither $C_6H_4Cl^+$ nor $ClC_6H_4S^+$ is observed. It is interesting to note that intact chlorothiophenol adsorbates are readily desorbed as $ClC_6H_4S^-$ in laser desorption experiments.[57] Note, too, that each of these surfaces shows a peak at m/z 18 (~20%) corresponding to $H_2O^{\bullet+}$, suggesting the availability of vacant adsorption sites and supporting the view that the surface is not highly ordered. Note also that electrochemical measurements[58] have confirmed the presence of defects in monolayers formed with small molecules, such as diphenyl disulfide, on a gold surface.

The strength of the sulfur−carbon linkage in the two classes of chemisorbate, CBM and CTP, may be responsible for the difference in intensity of the peaks due to chemical sputtering.

(57) Huang, J.; Dalgren, D. A.; Hemminger, J. C. *Langmiur* **1994**, *10*, 626.
(58) Bandyopadhyay, K.; Patil, V.; Sastry, M.; Vijayamohanan, K. *Langmuir* **1998**, *14*, 3808−3814.

For the CBM system, the C−S bond energy is estimated to be ∼60 kcal/mol (estimated from $C_6H_5CH_2-SH$), whereas the C−S bond energy for CTP is much higher, ∼85 kcal/mol (estimated from C_6H_5-SH).[59] The significant difference in bond energies clearly explains why a peak at *m*/*z* 125 ($ClC_6H_4CH_2^+$) was observed in the CBM system, while the corresponding ion $ClC_6H_4^+$ (*m*/*z* 111) was not detected in the CTP system.

CONCLUSIONS

The results presented above show that ion/surface chemistry is strongly influenced by the nature of the adsorbate including its structure (both connectivity and orientation). Appropriate reagent ions can distinguish the isomeric adsorbates under favorable conditions. It is postulated that the differences in reaction product abundance in the 4-CBM and 2-CBM monolayers are a consequence of the differences in accessibility of the aromatic chlorine and the difference in the ease of HCl elimination in one isomeric structure over the other. Whereas the HCl loss through rearrangement from a 2-CBM-derived fragment is more likely than from 4-CBM, $C_7H_5-Cr^+$ (*m*/*z* 141) is observed in increased abundance in the former. As far as $C_7H_5S-Cr^+$ and $C_7H_6S-Cr^+$ (*m*/*z* 173 and 174) are concerned, since chlorine is available at the surface in 4-CBM, these peaks are more intense in that case. The increase in intensity of $C_7H_5S-Cr^+$ ion with collision energy suggests that it is formed through the subsequent dissociation of $C_7H_6S-Cr^+$. The major result of this study, independent of the details of their rationalization, is that ion/surface reactive scattering can differentiate isomeric adsorbates.

(59) Lias, S. G.; Bartmess, J. E.; Liebman, J. F.; Holmes, J. H.; Levin, R. D.; Mallard, W. G. *J. Phys. Chem. Ref. Data* **1988**, *17*, Suppl 1.

ACKNOWLEDGMENT

T.P. acknowledges a Fulbright Fellowship and a Fulbright−Tata Travel grant. This work was supported by the National Science Foundation (Grant CHM-9732670).

Received for review April 19, 1999. Accepted May 3, 1999.

AC990402T